



## Investigation of the stall delay of a 5kW horizontal axis wind turbine using numerical method

Hsiao Mun Lee and Leok Poh Chua

School of Mechanical & Aerospace Engineering  
Nanyang Technological University  
50 Nanyang Avenue, Singapore 639798

Phone/Fax number:+65-82690125, e-mail: [leeh0071@e.ntu.edu.sg](mailto:leeh0071@e.ntu.edu.sg), [mlpchua@ntu.edu.sg](mailto:mlpchua@ntu.edu.sg)

**Abstract.** In this paper, a three-dimensional (3D) computational fluid dynamics (CFD) model is constructed to test a 5kW horizontal axis wind turbine HAWT that was designed using BEM method. It is found that the power coefficient of 0.38 determined by the 3D CFD model is higher than 0.34 obtained by the BEM method. The difference should be due to the stall delay in the rotation flow field of the wind turbine model, which was confirmed by the simulation results that the flow remain attached to the blade surface when wind velocity has reached 20m/s. The behaviours of the flow separation were also investigated under different wind speed in order to improve the performance design of the wind turbine blade.

### Key words

horizontal axis wind turbine, CFD, BEM method, wind tunnel

### 1. Introduction

The results obtained by BEM method using the two-dimensional (2D) experimental airfoil data are usually in good agreement with numerical simulation or field measurements for attached flow on the turbine blade surface. However, BEM method under-estimates the power output of turbine due to its 2D nature and does not consider the boundary layer induced on the rotating wind turbine blades which has further increased the lift and reduce the drag and thus delay the stall conditions [1]-[2]. Viterna and Corrigan [3] were the first to suggest that airfoil stall characteristics play an important role in causing these errors. The power output was always underestimated at lower tip speed ratio [4]. Some researchers examined the importance of stall delay in helicopters during forward flight which is useful in the research of future wind turbine design [5]-[7].

The effects of stall delay on 3D rotating blade have, therefore, a significant impact on the design of HAWT using BEM method. It is very important that the power

output of a wind turbine can be maximized and estimated precisely so that the turbine will not be over-loaded or under-loaded. In the present study, the power coefficient of the 5kW wind turbine that obtained by BEM method and numerical simulation were compared and separation flow of this turbine was examined by 3D CFD model.

### 2. Three-dimensional numerical simulation

The 5kW wind turbine has blade radius of 2.73m. Mesh generation was carried out using Gambit, only 120° periodicity was applied to computation domain in order to save the computational time and therefore, only one blade is modelled. There were 1,515,047 tetrahedral cells in the domain. A steady and uniform velocity was applied at the inlet with 1% turbulence intensity. A constant pressure distribution were applied at the outlet as shown in Figure 1. Smooth surface was applied on the nacelle and blade with no slip wall boundary configuration.

The simulation was carried out using Fluent software. The SST  $k\omega$  and SA turbulence models were used. Tests suggest that SST  $k\omega$  model gives superior performance for flow with adverse pressure gradient boundary, zero pressure gradient boundary and free shear layer [8] because this is a hybrid model which uses the standard model in the fully turbulent region far from the wall and uses  $k\varepsilon$  model in the near-wall region. All computation domains were set as rotating frame. Wind speeds in the negative Z-direction ranging from 6.67 to 60m/s were used for analysis while keeping the rotating speed of the rotor constant at 22rad/s. As such, the blade is rotating about the Z-axis in anti-clockwise direction in the absolute reference frame.

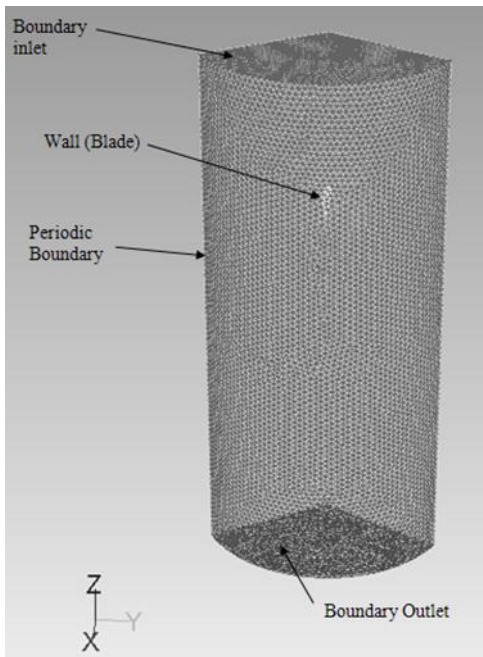


Fig. 1. 3D computational domain

### 3. Results and Discussion

#### A. Relative Velocity Vectors

Note that due to space constraints, not all wind speeds investigated are presented. The corresponding tip speed ratio (TSR) for wind speeds of 7.5, 10, 20 and 30m/s are 8,6,3 and 2 respectively. The relative velocity vectors of the blade at  $r/R=0.2$ , 0.5 and 0.9 are shown in Figures 2, 3 and 4 respectively. Note that the velocity vectors were obtained by taking the rotating speeds of the blade as the reference and the velocity vectors presented are distorted due to presenting the 3D vectors in 2D Y-Z plane. It can be observed that the air flows smoothly along the blade for the wind speed of 7.5 to 10m/s at  $r/R=0.2$  as shown in Figures 2 (a) and (b) respectively. When the wind speed increases to 20m/s, the flow is basically attached to the blade and only small circulation flow near the trailing edge on the suction side of the airfoil is observed in Figure 2 (c). When the wind speed increases to 30m/s, the flow separation has happened at 0.1c from the leading edge of the suction side and a big vortex can be observed in Figure 2 (d).

The similar phenomenon can be observed at  $r/R=0.5$  where the flow separation is happened at location closer to the leading edge when the wind speed reaches 20 and 30m/s as shown in Figures 3 (c) and (d) respectively. It can be found that when twist angle is decreasing from the hub to the blade tip, the flow separation is not likely to happen at higher radial locations. It is not unexpected that the flow is smoothly attached to the blade at  $r/R=0.9$  for all wind speeds as shown in Figure 4.

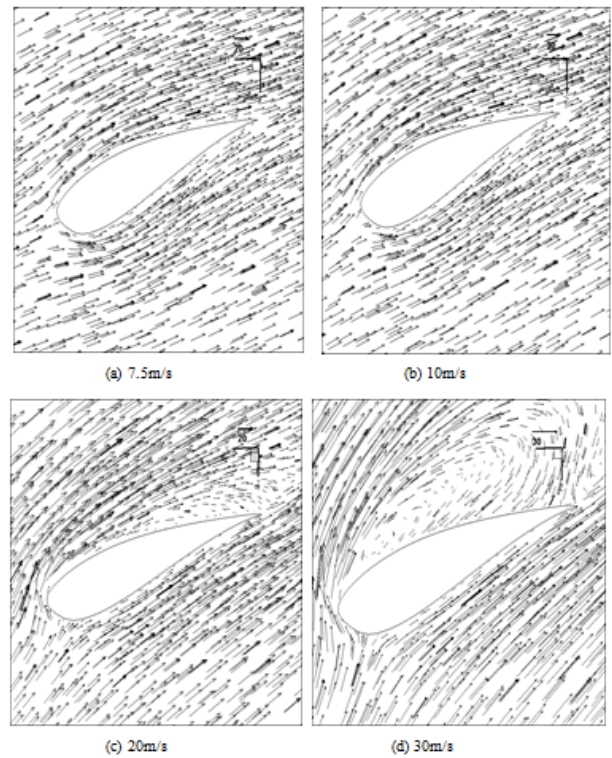


Fig. 2. Relative velocity vectors at radial station  $r/R=0.2$  at wind speeds of (a) 7.5m/s (b) 10m/s (c) 20m/s (d) 30m/s.

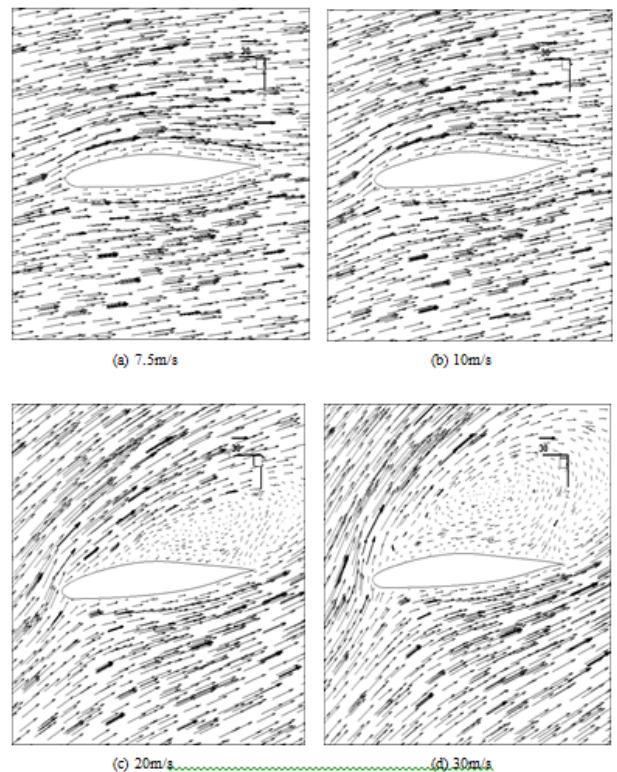


Fig. 3. Relative velocity vectors at radial station  $r/R=0.5$  at wind speeds of (a) 7.5m/s (b) 10m/s (c) 20m/s (d) 30m/s.

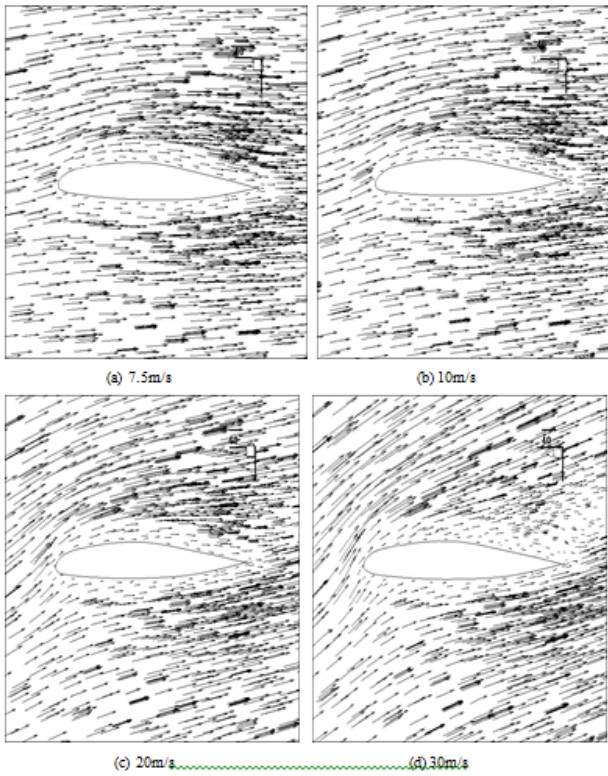


Fig. 4. Relative velocity vectors at radial station  $r/R=0.9$  at wind speeds of (a) 7.5m/s (b) 10m/s (c) 20m/s (d) 30m/s.

### B. Surface Limiting Streamlines

Streamlines limiting streamlines along the suction side of the wind turbine blade were generated as shown in Figure 5 to give a full picture of the velocity vectors which were presented earlier in Figures 2, 3 and 4 since limiting streamlines are often applied to depict surface flow status. Note that in the figure, the wind turbine blade is oriented from the root to tip along X-axis. It can be observed that the streamlines flows smoothly from the leading edge to trailing edge along the suction side of blade surface at 7.5 and 10m/s wind speed as shown in Figures 5 (a) and (b) respectively. As the wind speed reaches 20m/s, it can be seen from Figure 5 (c) that some streamlines from  $r/R=0.2$  onward has started to deviate from the leading edge to trailing edge by turning from about  $45^\circ$  to  $135^\circ$  and back to  $45^\circ$  till  $r/R=0.7$ . The location of turning which indicated the flow separation, has started from about the trailing edge to the upstream of about half of the in the figure. It can also be observed in the Figure 5 (d) that the flow starts to change direction from root region at 0.5c and become an obvious  $90^\circ$  clockwise turn till  $r/R=0.9$  at 0.9c when the wind speed increases to 30m/s. That is at this speed, the separation region starts much earlier from the root at 0.5c after the leading edge and ends at  $r/R=0.9$ , the flow seems following quite closely the profile of blade trailing edge as can be observed in the figure.

The flow remains smoothly attached to the blade surface at larger radial position i.e. from  $r/R=0.7$  to 1 and  $r/R=0.9$  to 1 at 20 and 30m/s as shown in Figures 5 (c) and (d) respectively. This is due to the effect of centrifugal force which pushing the separated flow radially outward. The radial motion of separated flow is expected to affect the

behavior of the boundary layer and to increase the lift force [9]. According to Lindenburg [10], motion of separated flow gives an additional negative pressure on the blade surface which has a stabilizing effect on the boundary layer. Therefore, the radially moving separated flow reattached back to the blade at larger radial positions.

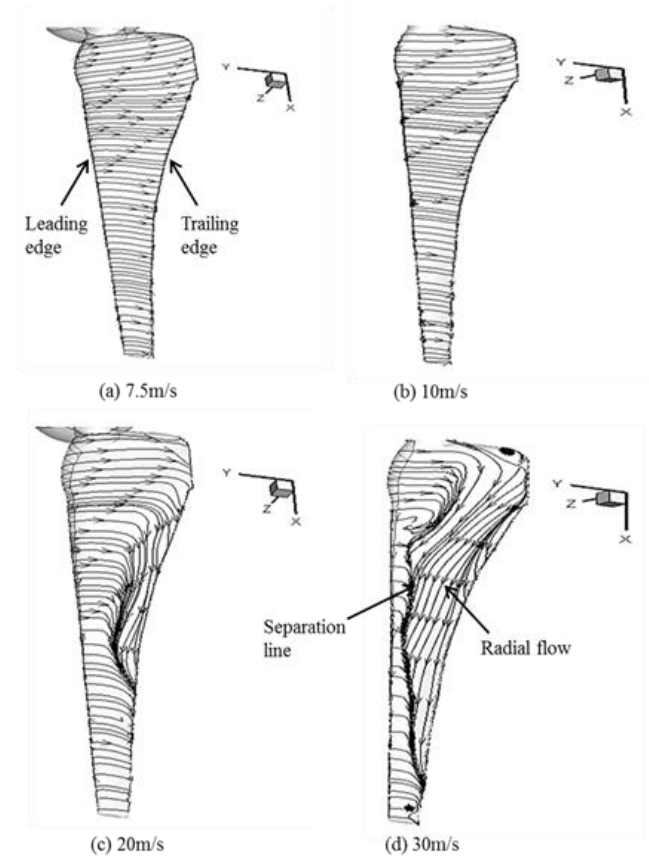


Fig. 5. Surface limiting streamlines (suction side) at wind speeds of (a) 7.5m/s (b) 10m/s (c) 20m/s (d) 30m/s.

### C. Comparison of BEM Method with CFD

Comparison of the power coefficient obtained by SA and SST  $k\omega$  turbulence model with BEM method is shown in Figure 6. The rated wind speed and rated power for this turbine is 10m/s and 5kW respectively. The maximum power coefficient that obtained by BEM method, SA and SST  $k\omega$  is 0.34, 0.34 and 0.38 respectively. SST  $k\omega$  model obtained higher power coefficient than BEM method for TSR ranging from 3 to 8. When the TSR is high, SA model obtained lower power coefficient than those from BEM method.

The differences between the results of the BEM method and CFD simulations are due to the key assumptions of the former that there are no aerodynamics interaction between different blade elements because the forces on each element are obtained independently and only determined by drag and lift coefficients. As discussed earlier in Section C, the wind have turned its direction from the leading edge to trailing edge by about  $90^\circ$  to X direction (Figure 5 (d)) at 30m/s, i.e. the flow separation has occurred. This has shown that there is an aerodynamics interaction between different blade

elements since the air is moving along the radial direction (same as X direction) of the blade.

BEM method is based on inviscid flow but the viscosity was included in both turbulence models. Furthermore, the power coefficient that obtained by BEM method is generally lower as compared to simulation results, this is due to stall delay phenomenon in 3D rotating flow where the wind remains attached to the blade surface at the root region even when the wind speed is as high as 20m/s. Rotation resulted in dynamic pressure increases along the blade radial direction toward the tip. The variation of dynamic pressure along the blade is expected to induce a radial velocity to the flow. The radial velocity component results in the appearance of Coriolis force which directed toward the trailing edge of the blade. The Coriolis force induces a positive pressure gradient and thus delays flow separation [11].

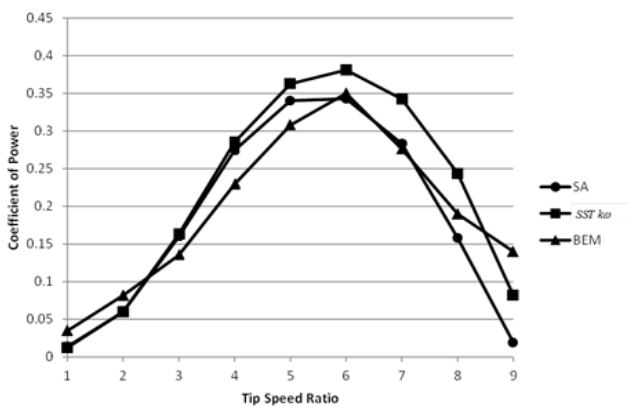


Fig. 6. Coefficient of power versus tip speed ratio

#### 4. Conclusions

A 3D CFD model is built to examine the stall delay phenomenon of a 5kW horizontal axis wind turbine. The flow remains attached to the blade surface when the wind speed has increased to 20m/s at the root region of the blade. It is also shown that the power output predictions from BEM method are generally lower than those obtained from 3D CFD simulation using SST  $k\omega$  turbulent model. BEM method is based on inviscid flow, but the viscosity was included in both turbulence models. Furthermore, the difference should be due to the stall delay in the rotation flow field of the wind turbine model, which was confirmed from the 3D simulation results that the flow remains attached to the blade surface at the root region when wind velocity reached 20m/s.

#### References

[1] Clausen, P. D., Piddington, D. M. and Wood, D. H., An experimental investigation of Blade Element Theory for wind turbine, Part 1, mean flow results, *Journal of Wind Engineering and Industrial Aerodynamics*, 1987, Vol. 25, pp 189-206.  
 [2] Wood, D. H., Some effects of finite solidity on the aerodynamics of horizontal-axis wind turbines, *Journal of Wind Engineering and Industrial Aerodynamics*, 1987, Vol. 26, pp 255-273.  
 [3] Viterna, L.A. and Corrigan, R.D., Fixed pitch rotor performance of large horizontal axis wind turbine, DOE/NASA

Workshop On Large Horizontal Axis Wind Turbines, Cleveland, OH, July, 1981, pp 69-85.  
 [4] Tangler, L., Comparison of wind turbine performance prediction and measurement., *Solar Energy Research Institute*, 1981, Vol. 2, pp 573-585.  
 [5] McCroskey, W. J., and Yaggy, P. F., Laminar boundary layers on helicopter rotors in forward flight, *AIAA Journal*, 1968, Vol. 6, pp 1919-1926.  
 [6] Velkoff, H. R., Blaser, D.A. and Jones, K.M., Boundary-layer discontinuity on a helicopter rotor blade in hovering, *Journal of Aircraft*, 1971, Vol. 8, pp 101-7.  
 [7] Young, W. H. and William, J. C., Boundary-layer separation on rotating blades in forward flight, *AIAA Journal*, 1972, Vol. 10, pp 1613-19.  
 [8] Versteeg, H. K. and Malalasekera, W., *Computational Fluid Dynamics (the finite volume method)*, 2007, Prentice Hall.  
 [9] Breton, S., Study of the stall delay phenomenon and of wind turbine blade dynamics using numerical approaches and NREL's wind tunnel tests, 2008, Norway University Science and Technology.  
 [10] Lindenburg, C., Investigation into rotor blade aerodynamics, 2003, ECN-C-03-025, Netherlands.  
 [11] Hu, D., Hua, H. and Du, Z., A study on stall-delay for horizontal axis wind turbine, *Renewable Energy*, 2006, Vol. 31, pp 821-836.